Passive Filtration of Airborne Particles from Buildings Ventilated by Natural Convection: Design Procedures and a Case Study at the Buddhist Cave Temples at Yungang, China

Christos S. Christoforou , Lynn G. Salmon & Glen R. Cass

Passive Filtration of Airborne Particles from Buildings Ventilated by Natural Convection: Design Procedures and a Case Study at the Buddhist Cave Temples at Yungang, China

Christos S. Christoforou, Lynn G. Salmon, and Glen R. Cass[*]
ENVIRONMENTAL ENGINEERING SCIENCE DEPARTMENT,
CALIFORNIA INSTITUTE OF TECHNOLOGY, PASADENA, CA 91125

ABSTRACT. Air exchange between interior spaces and the outdoor atmosphere can occur due to a variety of processes, including wind-driven flows and natural convection-driven flows. As air is exchanged with the outdoors, airborne particles can be brought inside. Depending on the use of the indoor space, the presence of particles in indoor air could be a nuisance to the occupants or could be damaging to materials kept indoors. While one obvious solution to such problems is to install a mechanical air filtration system, that is not always practical. In particular, the character of some historical houses and some archaeological sites would be degraded by the presence of a mechanical air distribution system, and in some parts of the world the reliable electrical power supply needed for such a filtration system may not be available.

In the present paper we consider principles for the design of passive filtration systems in which air motion through the filter material is induced by a natural convection flow rather than by a mechanical fan. A fluid mechanical model first is described for predicting the air flow through an interior space that acts as a thermal siphon. The effect of placing filter material in the path of such air flows is examined next. The indoor-outdoor air quality model of Nazaroff and Cass (1989a) is matched to the natural convection air exchange model, and calculations are performed to determine the relationship between the outdoor particle size distribution and indoor particle size distributions and particle deposition rates given a passive filtration system.

Example calculations are worked for the case of a passive particle filtration system that could be installed to protect the interior of the Buddhist cave temples at Yungang, China. These are a collection of manmade cave temples dating from the 5th century AD, now situated in the middle of one of China's largest coal-mining regions with its accompanying air pollution problems.

INTRODUCTION

Mechanical air filtration systems are widely used to control indoor air quality through the removal of particles present in outdoor air. Such systems can be used to protect occupants from adverse health effects caused by breathing polluted air. Also, these systems can be used to protect against damage to materials. For

---

[*]Corresponding author.

example, particle deposition onto various objects displayed inside museums can adversely affect the visual qualities of such objects (Nazaroff and Cass 1991; Hancock et al. 1976), and particle filtration systems provide one means of averting such damage.

In the case of certain historical structures or archaeological sites, installation of elaborate mechanical air filtration systems is not advised because it would alter the historical context of the building. Such a filtration system would require its own mechanical equipment housing, ductwork, filter material, and other necessary accessories which would alter the physical appearance of the site. Furthermore, in developing countries or places remote from electrical power, a mechanical air filtration system may not be practical at all, or would require the installation of electrical generators, thus further complicating the issue.

One alternative would be to devise passive air filtration systems. Passive filtration systems are those which employ ambient pressure differences to drive particle-laden air streams through filters. One can envision several types of systems, for example, air can be driven through the filters by wind fluctuations or by density differences due to indoor/outdoor temperature differences. The choice between systems will depend on the particular physical situation at hand. The purpose of this article is to describe an approach to the design of passive filtration systems that rely on density differences that are due to indoor/outdoor temperature differences to move the air stream through filters.

A condition is examined in which a structure, with massive masonry walls and openings to the outdoors at several elevations, experiences a temperature difference between the interior walls and the outdoor air. These temperature differences lead to natural convection air flows along the interior walls, which in turn produce air exchange between the interior of the structure and the outdoor atmosphere. Such a structure is depicted schematically in Figure 1a.

Conditions under which this natural convection flow can be used to drive particle-laden air through filters as air enters the structure are then defined. Mathematical modeling procedures are developed that account for air exchange with the outdoors, particle filtration from that air flow, prediction of indoor particle size distributions, chemical composition given those parameters in the outdoor air, and prediction of particle fluxes to indoor surfaces that may require protection (e.g., museum collections).

Procedures for the design of such passive filtration systems are illustrated by application to the filtration of particles from the atmosphere at the Buddhist cave temples at Yungang, China. This is one of the few locations, if not the only location, where actual data are available on a natural convection flow of particle-laden air through an indoor/outdoor setting, having sufficient detail regarding particle size distributions, temperature differences, and air flow rates, that it can be used to illustrate the more general design procedure.

PROBLEM FORMULATION

The first step in developing a passive filtration system for a structure is to be able to calculate the rate at which air enters such a structure and subsequently to calculate how this air exchange rate is changed in the presence of additional pressure drops, which may be added in the air flow path in the form of filters and other obstructions.

Air exchange between the interior of a structure and the outdoors is modeled according to the procedure described by Christoforou et al. (1996a). Assume initially that the structure can be modeled as a single chamber with two openings to the outdoors, one at ground level and one at an upper level. A simple schematic diagram of such a structure is shown in Figure 1a. A natural convection flow occurs along the walls due to wall and air temperature differences. When warm air flows into a structure, it enters through the upper level opening (position 2 in Figure 1a). The air is cooled as it flows down the walls; cool air accumulates in the room and then flows
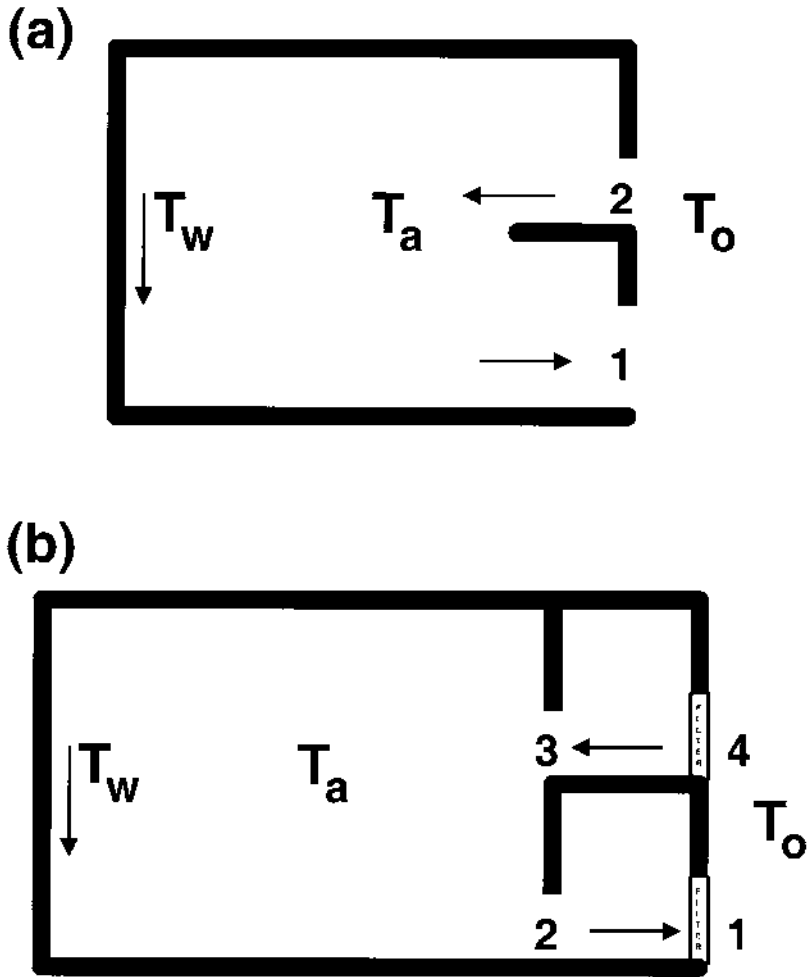
FIGURE 1. (*a*) Vertical cross section of a simple structure with doors or windows at two elevations and (*b*) a more complex building with several sets of exterior and interior doors and windows in series, and showing filter placement in openings in the outer shell of building at positions 1 and 4. T_o is the outdoor air temperature, T_a is the indoor air temperature in the core of the building, and T_w is the temperature of the interior walls of the building. For a massive stone structure with cold walls, air will flow in the direction shown when $T_o > T_w$. If the building interior and its walls are warmer than the outdoor air, flow will be in the opposite direction.

out of the ground-level entrance to the structure (position 1 in Figure 1a). The simultaneous convection and heat transfer problem within such a structure can be described by the following set of equations:

$$\frac{d}{dt}(\rho_a V) = \rho_o U_2 A_2 - \rho_a U_1 A_1 \tag{1}$$

$$\frac{d}{dt}(\rho_a V c_v T_a) = \rho_o U_2 A_2 c_p T_o - \rho_a U_1 A_1 c_p T_a$$

$$- \sum_{i=1}^{n} h_i S_i (T_a - T_w) \tag{2}$$

$$\frac{1}{2}\rho_o U_2^2 C_L + \frac{1}{2}\rho_a U_1^2 C_L = gH(\rho_a - \rho_o) \tag{3}$$

where ρ_a is the mass density of air inside the structure, ρ_o is the mass density of air outside the structure, T_a and T_o are the temperatures of the air inside the structure and the air outdoors, respectively, T_w is the temperature of the interior surfaces of the walls of the structure, U_1 and U_2 are the air velocities through the openings between the outdoors and the inside of the structure at positions 1 and 2 in Figure 1a, respectively, h_i is the heat transfer coefficient for flow over the ith surface inside the structure, c_p is the specific heat of air measured at constant pressure, c_v is the specific heat of air measured at constant volume, A_1 and A_2 are the cross sectional areas of the openings (positions 1 and 2 in Figure 1a), S_i is the surface area of the ith surface inside the structure, V is the volume of the structure, C_L is the loss coefficient for flow through the openings at positions 1 and 2 in Figure 1a, H is the elevation difference between the air entering and exiting the structure, and g is the acceleration due to gravity. Equation (1) is a continuity equation, Equation (2) describes energy conservation, and Equation (3) represents the balance between the pressure drops in the air path versus density differences acting on the height of the air column between the entering and exiting air paths, respectively.

By assuming that $\rho_a \approx \rho_o \approx \rho$ except that $\frac{\rho_a - \rho_o}{\rho_o} \neq 0$, and also $\frac{\rho_a - \rho_o}{\rho_o} \approx \frac{T_o - T_a}{T_o}$, Equations (1)–(3) are simplified as described by Christoforou et al. (1996a). For the case where cold air enters at ground level and flows up the warmer walls of the structure, a corresponding set of equations can be written. Given building dimensions plus measured values for the outdoor air temperature and wall temperature, the unknown air velocities through the openings into the structure, U_1 and U_2, as well as the indoor air temperature, T_a, can be determined by integrating the unsteady state form of the simplified governing equations numerically. The air flow through the structure is determined by multiplying either U_1 or U_2 by the cross sectional area of the openings through which the air enters or leaves the structure. An illustration of the results of a computer program for performing such calculations and expressions for estimating heat transfer coefficients are provided by Christoforou et al. (1996a).

Once particle-laden outdoor air has been drawn into the structure, airborne particles will deposit onto various surfaces. The computer-based indoor air quality model of Nazaroff and Cass (1989a) is used to describe the time series of particle deposition onto surfaces within the structure. The structure is represented by a single well-mixed chamber model in which particles are advected through the structure in the presence of indoor sources and particle deposition,

$$V \frac{d}{dt}(C_{aj\,k}) = C_{oj\,k} f_{oa} + E_{aj\,k}$$
$$- C_{aj\,k} \sum_i S_i v_{d_{ij\,k}} - C_{aj\,k} f_{oa} \quad (4)$$

where $C_{aj\,k}$ and $C_{oj\,k}$ are the concentrations of chemical component k in particles of size j in air inside (a) or outside (o) the structure, respectively, $E_{aj\,k}$ is the emission rate of new particles of composition k and size j due to activities within the structure, f_{oa} is the volumetric flux of air flowing from outside to inside the structure (flow in = flow out in this case), S_i is the surface area of the ith surface and $v_{d_{ij\,k}}$ is the deposition velocity for particles containing component k in size j to the ith surface within the structure. Particle deposition velocities to horizontal and vertical surfaces within the structure are calculated for laminar or turbulent natural convection flows along the walls, for deposition due to homogeneous turbulence in the core of the room, as well as for deposition to horizontal surfaces by both gravitational sedimentation and convective diffusion. The equations used for computing these deposition velocities are given in Christoforou et al. (1996b) and Nazaroff and Cass (1987, 1989a,b). The deposition velocity due to gravitational sedimentation is corrected using a dynamical shape factor for mineral dust particles that accounts for the irregular shape of the coarse

dust particles encountered. That shape factor is the ratio of the settling velocity of a sphere to that of an irregularly shaped particle of the same volume and density; numerical values for mineral dusts are tabulated by Davies (1979).

The natural convection air flow model that incorporates particle deposition mechanics calculations just described is ideally suited to study passive filtration possibilities because that model can be modified to predict the changed air flow that will occur as extra pressure drops are added to the air flow path in the form of new filter material or in the form of a more complex series of interior doors. A schematic diagram showing the relative placement of filter material in the outer wall panels of a more complex structure is shown in Figure 1*b*. An illustration of how the model changes as additional pressure drop terms are added to the flow path of the air entering the structure follows.

Consider the placement of filter material over the air flow entrance and exit points for a build-ing; personnel may still enter and leave the building through doors that normally remain closed. One possible filter material that may be used is type GSB-30, produced by Minnesota Mining and Manufacturing Co. Particle collection efficiency curves for that material, supplied by the manufacturer, are shown in Figure 2 and indicate high single pass filtration efficiency for coarse particles larger than 10 μm in diameter and reasonably good filtration efficiency for smaller particles when compared to many commercial HVAC filter materials. One major advantage of this filter material is its very low pressure drop as a function of face velocity. The pressure drop across this filter material is specified to vary linearly as a function of the air velocity through the filter for velocities under 0.5 m s^{-1} and from the manufacturer's specifications (Minnesota Mining and Manufacturing, 1993) we can infer that
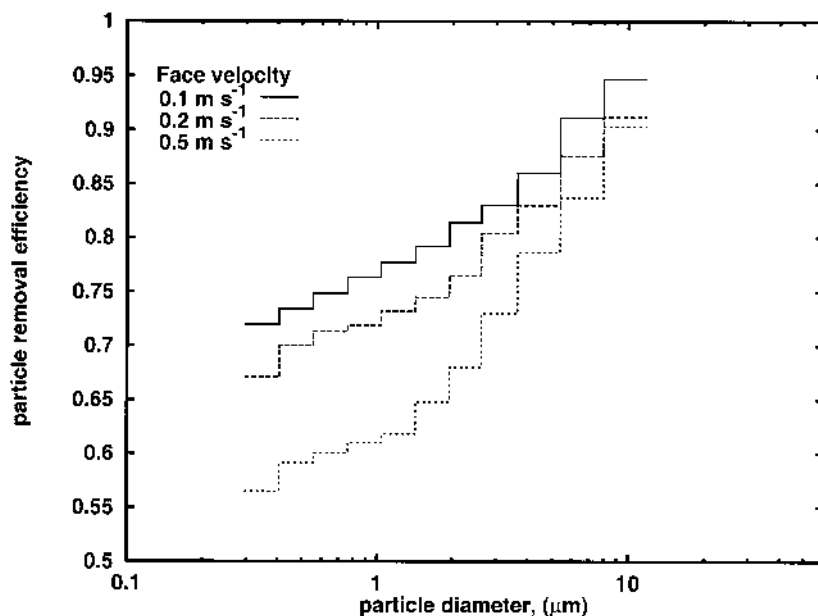
$$\Delta P = \kappa u \qquad (5)$$

FIGURE 2. Efficiency curves for 3M's GSB-30 filter material as a function of particle size and face velocity. Data are according to the manufacturer's specifications.

where ΔP is the pressure drop in Pa and u is the face velocity through the filter in m s^{-1}. κ is a constant that depends on the filter used and equals 15.1 Pa m^{-1} s for filter type GSB-30 according to the manufacturer's specifications.

The system of Equations (1)–(3) is used to solve for the flow of air through the structure described in Figure 1b but this time the equation that balances pressure drops in the flow path against the indoor/outdoor air density differences is changed. Additional pressure drop terms are now present in the equation corresponding to former Equation (3) that reflect losses that occur while the air passes through both interior doorways at positions 2 and 3 in Figure 1b as well as through filter material present in the surface of the building at ground level and in the upper level surfaces of the building at positions 1 and 4 in Figure 1b:

$$\Delta P_t = (R_1 + R_2 + R_3 + R_4)Q_t \qquad (6)$$

where $\Delta P_t = gH(\rho_a - \rho_o)$ is the total pressure drop available to drive air through the system, R_1 and R_4 are the resistances to the flow as air passes through the cracks and filters in the surface of the building (assuming the exterior shell of the structure will not be airtight, but rather that some amount of outdoor air will leak unfiltered into the structure from the outdoors), R_2 and R_3 are the resistances to the flow as air passes through the interior doorways, and Q_t is the total volumetric flow of air through the structure. The pressure drop, as air passes through the cracks or other openings in the building shell at the ground floor level, for example, must be the same as the pressure drop across the filter material located in the building wall panels at the ground floor level. By analogy to electrical circuit systems

$$R_1 = \frac{R_c R_f}{R_c + R_f} \qquad (7)$$

where R_f is the resistance to flow due to air passage through the filter material and R_c is the resistance to flow due to air passage through the cracks or other openings in the building shell.

From Equation (5),

$$R_f = \frac{\kappa}{A_f} \qquad (8)$$

where A_f is the surface area of the filter material used and

$$R_c = \frac{1}{2}\rho_o C_L \frac{Q_c}{A_c^2} \qquad (9)$$

where Q_c is the air flow rate through the cracks and openings in the building shell at that level, A_c is the area of those cracks and openings, and C_L is the loss coefficient for flow through those cracks and openings (the openings are taken to be rectangular and C_L is taken to be 1.5, as for induction of air into a building from outdoors [Jennings and Lewis 1965], and for flow through a square edged orifice [Sabersky et al. 1989]).

For resistances R_2 and R_3, expressions similar to Equation (9) may be written, with the exception that now the flow would be equal to Q_t in both instances and the areas are those of the two interior doorways within the structure. Also, R_4, the resistance to flow through the cracks in the building shell and filters at the upper level of the shelter, may be written in exactly the same way as R_1, noting that the total flow, Q_t, may be split in different proportions between flow through the cracks and flow through the filters. The relationship between Q_t, Q_c, and Q_f may be obtained by noting that the pressure drop across a given set of cracks and openings in the building shell must be equal to the pressure drop across the filter material that is in parallel with those cracks:

$$\kappa \frac{Q_f}{A_f} = \frac{1}{2}\rho_o C_L \frac{Q_c^2}{A_c^2} \qquad (10)$$

where Q_f is the volumetric air flow rate through the filter, and all other symbols are as previously defined. Also,

$$Q_t = Q_f + Q_c \qquad (11)$$

All resistance terms can then be substituted into Equation (6), which contains the unknown Q_t, as well as the density of the air, both outdoors

and inside the structure. Also, the simplified form of Equation (2) can be rewritten as

$$\rho c_v V \frac{d}{dt}(T_a) = \rho c_p Q_t(T_o - T_a)$$

$$- \sum_{i=1}^{n} h_i S_i(T_a - T_w) \quad \text{(12)}$$

As seen in Equation (6), the value of Q_t is a function of ρ_a, which in turn is a function of T_a. At each time step in the solution of Equation (12) the value of Q_t is updated by solving Equation (6).

The case for which there are no cracks at all in the building shell is more straightforward, as resistances R_1 and R_4 can then be written in a manner similar to Equation (8), and the resulting system of equations is easier to solve.

APPLICATION: THE BUDDHIST CAVE TEMPLES AT YUNGANG

The Yungang Grottoes are a collection of Buddhist devotional caves carved into the side of a cliff, dating from the 5th century A.D., outside the small village of Yungang, in northern Shanxi province, China. The results of experiments conducted at the Yungang Grottoes, reported previously (Christoforou et al. 1994; Salmon et al. 1994), show that the outdoor airborne particle concentrations at Yungang are very high, averaging 508 μg m^{-3} over an annual period in 1991–1992. Deposition of particles occurs onto horizontal surfaces within the caves largely due to gravitational sedimentation. The result is that the horizontally-oriented surfaces of the more than 50,000 sculptures within the grottoes can become noticeably soiled within a matter of hours and can become covered by the first complete monolayer of deposited dust within a matter of months. Over a period of five years, deposits as deep as 0.8 cm and with mass loadings as high as 5 kg m^{-2} have been measured to accumulate on the statuary within these caves (Christoforou et al. 1994). The challenge faced by the present example calculations is to determine the effectiveness of a passive filtration system that could be built to protect the interior of these cave temples from the high particle concentrations present outdoors.

Figure 3 shows a schematic diagram of one of the caves at Yungang, Cave 6. The cave walls, indicated by the shaded areas of Figure 3, are analogous to the walls of the massive stone building discussed when formulating the passive filtration problem. Two small rectangular entrances through the rock face of the cliff exist at positions 2 and 3 in Figure 3. To the right of the cave rock walls is a small wooden temple structure built over the entrance to Cave 6. Historically, the outside surface of that wooden structure has consisted of many narrow wooden door panels with wooden lattice work backed by paper windows. There is a massive pair of main entrance doors at ground level that traditionally are left open during the day but are closed at night. Door panels at the upper floors of the wooden temple structure often are left ajar as well. One possible design for a passive filtration system for a cave at Yungang involves closing the open doors at the cave temple accompanied by replacement of the paper in the windows by filter material, which is the condition shown schematically in Figure 3. Also shown in Figure 3 are the relevant parameters pertaining to the application of the model to Cave 6. The values of those parameters are given in Table 1. Most importantly, the large range of outdoor air temperatures compared to the nearly stable temperatures of the rock walls should be noted; it is the cycling of the outdoor air temperature relative to the indoor wall temperature that will drive the air flow through this system.

On April 15–16, 1991, a very detailed two-day long experiment was conducted at Yungang to gather data on the time series of particle concentration and fluxes over short averaging times specifically for the purpose of evaluating the performance of the present model for Cave 6. Christoforou et al. (1996a,b) describe more fully the measurements made. Briefly, the following data were gathered:
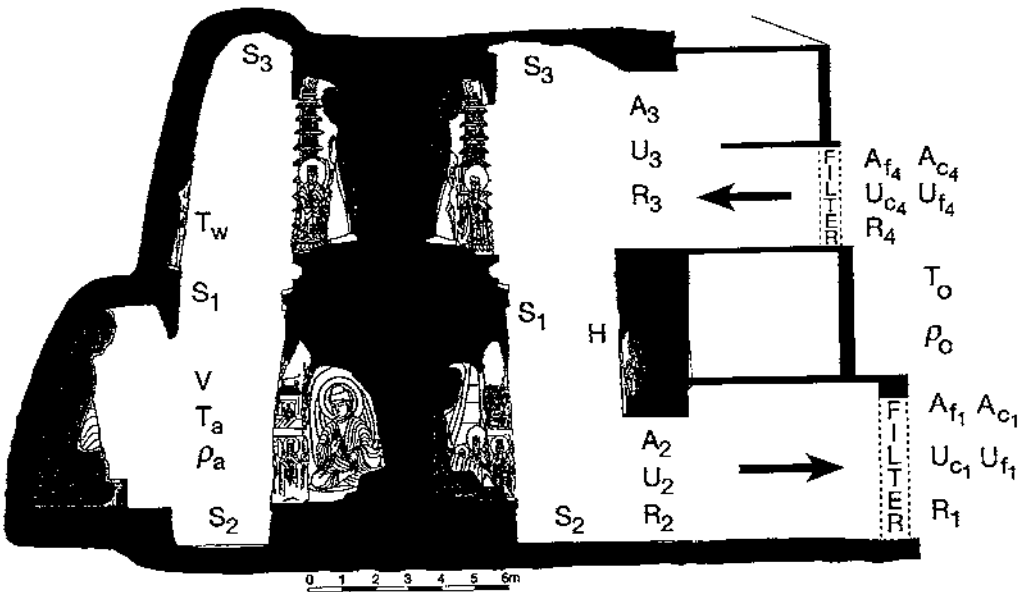
FIGURE 3. Schematic diagram of Cave 6 at Yungang. Symbols are as defined in the text and in Table 1.

TABLE 1. Characteristics of Cave 6 at the Yungang Grottoes.

Symbol	Description	Cave 6
T_w	indoor cave wall temperature; range April 15–16, 1991, °C	4.2–5.2
T_o	outdoor air temperature; range April 15–16, 1991, °C	−1.6–12.0
S_1	wall area, m^2	1370
S_2	ceiling area, m^2	163
S_3	floor area, m^2	179
V	volume, m^3	2222
Z	physical height of the cave, m	15
H	elevation difference between entering and exiting critical fluid streamline, m	9.25
A_{1a}	cross-sectional area of openings in building shell downstairs, front door open, m^2	4.8
A_{1b}	cross-sectional area of openings in building shell downstairs, front door closed, m^2	0.46
A_2	cross-sectional area of entrance through rock walls at ground level, m^2	11.82
A_3	cross-sectional area of opening in rock wall at 3rd plus 4th floor level, m^2	21.12
A_4	cross-sectional area of openings in building shell upstairs, m^2	4.2

1. Outdoor and indoor airborne particle concentrations and size distributions over consecutive 4-h periods,
2. indoor particle deposition fluxes onto both vertical and horizontal surfaces over consecutive 4-h periods,
3. continuous measurements of wall and air temperatures inside the cave and outdoor air temperatures,
4. air exchange rates measured by thermoelectronic air velocity probes, perfluorocarbon tracer methods and hand-held mechanical air velocity meters.

Verification of the ability of the natural convection model of Equations (1)–(3) to predict the air exchange rates through Cave 6 prior to the installation of any filter material given only the cave temple dimensions, time series of interior wall temperatures and time series of outdoor air temperatures is provided by Christoforou et al. (1996a). Over the course of this experiment outdoor air temperatures ranged from a high of $12.0°C$ to a low of $-1.6°C$. The Cave 6 air exchange model correctly calculates the cooling of that outdoor air during the day through heat transfer with the cave walls, as well as the warming of the outdoor air that enters the cave in the middle of the night, as seen in Figure 4a. Density differences between the indoor air and the air outdoors lead to air motion through the cave entrances. In Figure 4b the air exchange rate predicted by the heat transfer model is compared to air exchange rate measurements made successively during these experiments by perfluorocarbon tracer (PFT) techniques as well as by hand held mechanical velocity meters. A positive air exchange rate in Figure 4b indicates predicted flow into the cave through the ground level entrances (e.g., at night) while a negative air exchange rate indicates flow out of the ground level entrances during the day. Over the two-day period studied, PFT measurements indicate an average of the absolute value of the air exchange rate equal to $1.80 \, m^3 \, s^{-1}$ compared to an average air exchange rate of $1.65 \, m^3 \, s^{-1}$ predicted by the heat transfer model.

The combined model of Equations (1)–(4) is based on the dimensions of the structure, the thermodynamic properties of air, measured wall and outdoor air temperatures, measured particle size and concentration, plus heat transfer coefficients and loss coefficients for orifice flows that are straight from the mechanical engineering literature; there are no free parameters in the model. The ability of the model to predict indoor particle concentrations, particle size distributions, and particle fluxes to surfaces given the temperature data plus data on outdoor particle size and concentration is presented by Christoforou et al. (1996b). Additional model verification results are given in Figure 5. The predicted airborne particle number distribution inside Cave 6 averaged over the two-day experiment is shown in Figure 5a. Over the range of particle sizes larger than 2.3 μm diameter, that predicted size distribution can be compared to the measured airborne particle size distribution within Cave 6 as determined by automated optical microscopy applied to particle samples collected by filtration onto Millipore filters. From the particle deposition model, the projected cross sectional area, A, of depositing particles can be calculated and graphed as a surface area coverage rate (m^2 covered by deposited particles per m^2 of horizontal surface of the statues per unit time), as shown in Figure 5b. That surface area coverage rate is in reasonable agreement with values measured by automated optical microscopy applied to deposition samples collected on glass slides during the April 15–16, 1991 experiments, as seen in Figure 5b.

The particle deposition model of Christoforou et al. (1996b) now can be applied to study the effect of alternative passive filtration system designs. To begin this study, a "base case" is established that describes the particle deposition problem at Cave 6 as it would exist if the wooden temple structure in front of that cave temple were removed. This case provides an important point of reference because 18 of the 20 major caves at Yungang lack a wooden temple structure in front of their entrances at present. The flow restrictions caused by the wooden temple structure
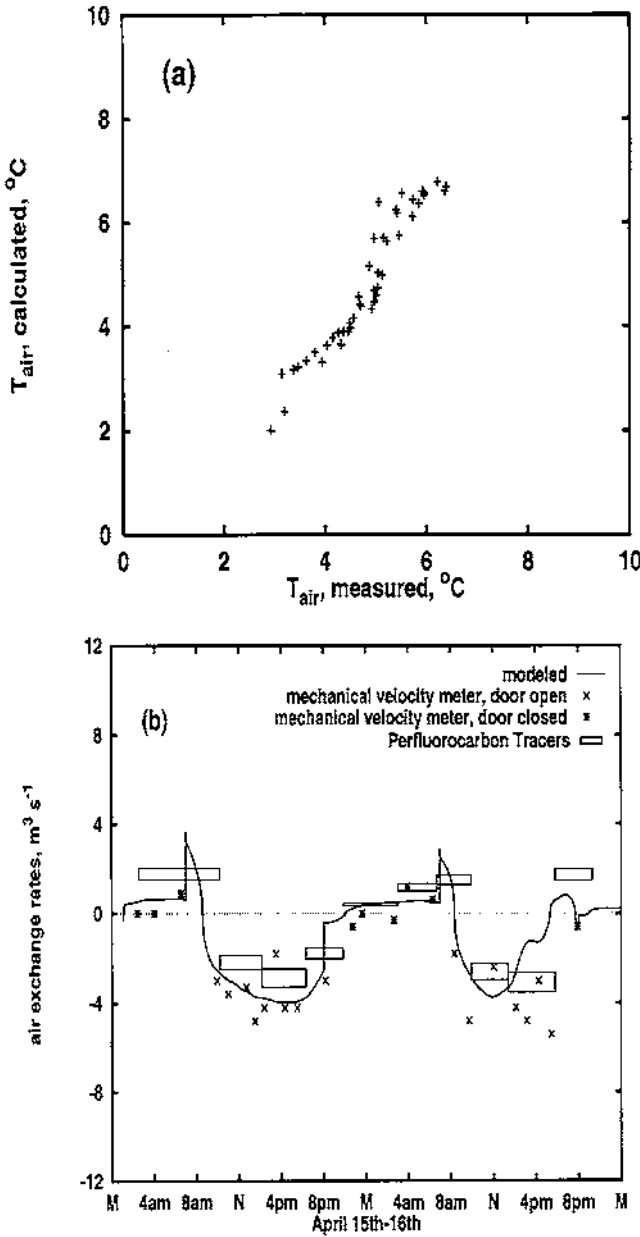
FIGURE 4. Performance of the air exchange model for Cave 6. (*a*) Predicted near-wall air temperature in Cave 6 compared to measured temperature. Comparisons are made every 60th minute over the two day period of April 15–16, 1991. (*b*) Volumetric air flow through Cave 6 predicted by the model compared to both perfluorocarbon tracer (PFT) measurements of air exchange rates and air exchange rates inferred from velocity measurements by a hand-held mechanical air velocity meter (Christoforou et al. 1996a). A positive air exchange indicates flow into the ground level entrance to Cave 6 (e.g., at night) while a negative air exchange rate indicates flow out of the ground level entrance to the cave (e.g., during the day).

are removed from the model of Christoforou et al. (1996b) producing a simpler interior space more like that in Figure 1 and the model is rerun given measured temperatures and outdoor particle sizes and concentrations observed on April 15–16, 1991. Given uncontrolled base case conditions and no wooden shelter in front of Cave 6, particle deposition fluxes onto horizontal surfaces within the interior of that cave temple would average 262 mg m^{-2} d^{-1} as seen in case 1
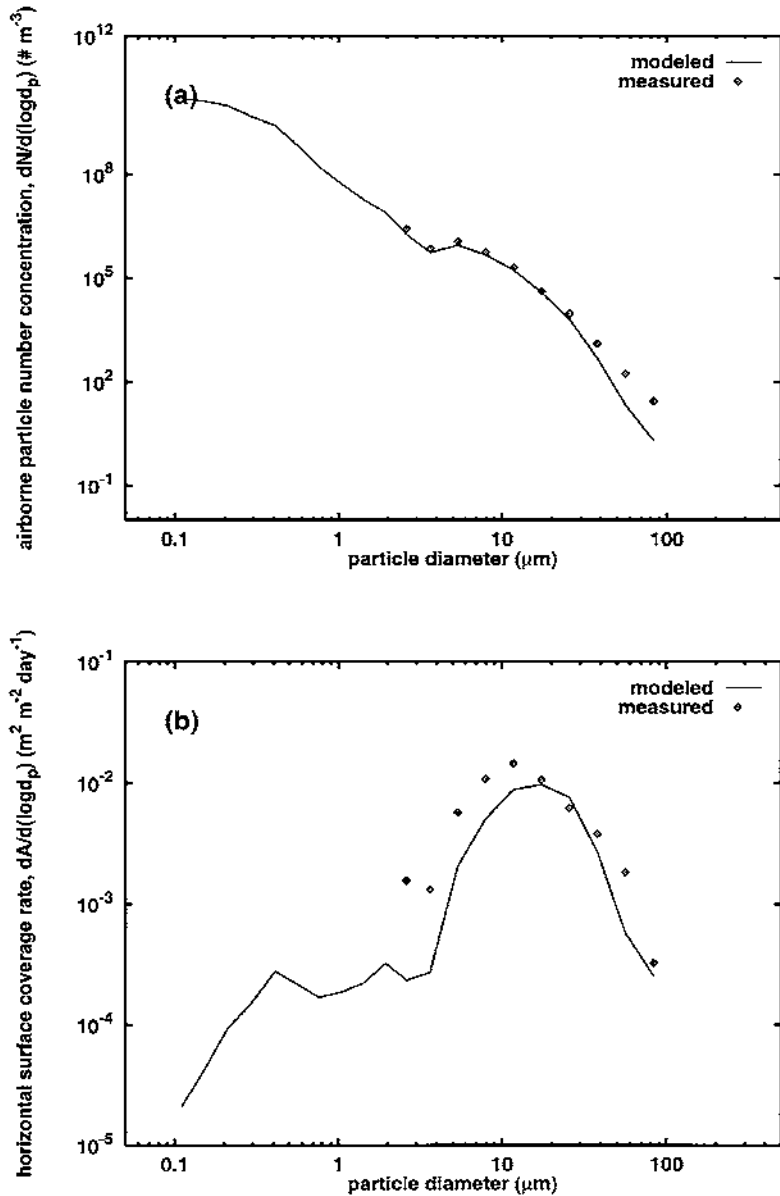
FIGURE 5. Model performance April 15–16, 1991: (*a*) Airborne particle number distribution inside Cave 6 average over the two-day period. (*b*) Predicted rate of coverage of horizontal surface area within Cave 6 by deposited particles as a function of particle size.

of Table 2.   Under these circumstances and given present outdoor pollutant levels at Yungang, it would take only one quarter of a year for all horizontal surfaces inside the cave to accu-

mulate a full monolayer of dark deposited dust, as shown in Table 2. For the purposes of the present discussion, a full monolayer coverage by dust is deemed to occur once particles hav-

TABLE 2. Effect of alternative passive filtration system designs on reducing the particle mass flux to horizontal surfaces within a cave temple the size of Cave 6 at the Yungang Grottoes[†]

	Air Flow through Cave Temple (m^3 min^{-1})	Mass Deposition to Horizontal Surfaces (mg m^{-2} day^{-1})	Percent Remaining Relative to Base Case (1)	Time to 100% Coverage by Particles (Years)
Base Case				
(1) Temple front removed	317	262	–	0.28
(2) Historical case: temple front in place	99	139	53	0.47
Tightening up the wooden building				
(3) Closed doors[a]	26	50	19	1.0
Filter material installed in place of paper windows				
(4) Building still leaks[b,c]	34	45	17	1.2
(5) Building has no leaks[b,d]	6.3	3.4	1.3	9.0
Maximum amount of filter material installed				
(6) Building has no leaks[e]	86	7.5	2.9	6.3

[†] Values shown are averages of model predictions over the two day period of April 15–16, 1991, for which data are available to drive the deposition model. As discussed by Christoforou et al. (1996b), deposition rates under annual average conditions are about 4 times higher than under April 15–16, 1991, conditions; deposition fluxes shown above should be scaled upward proportionately and the times to reach 100% coverage by particles should be divided by a factor of 4 when considering time periods that approach a year or larger.

[a] The only control measure in this case is to ensure that the doors at the ground floor level as well as balcony doors and windows on the upper floors remain closed at all times.

[b] Filter material with low pressure drop characteristics is installed on the available window panels on both the ground floor and the 3rd floor level in the place of the existing paper windows. The pressure drop and efficiency characteristics of 3M's filter type GSB-30 have been used in these calculations (see Figure 2).

[c] The doors on the ground floor as well as windows and balcony doors on the upper floors are assumed to remain closed at all times, but there is infiltration of air through cracks around the doors and windows of the building shell. Calculations show that 71% of the total mass of air that enters the cave does so through the cracks. Filter area both on the ground floor and the third floor level totals 2.56 m^2 at each level.

[d] In this case the cracks in the building shell have been caulked and all air entering the cave temple must pass through the filter material. Filter area both on the ground floor and the 3rd level totals 2.56 m^2 at each level.

[e] Same as (d) except now the filter material has been increased: 55.4 m^2 filter surface area is supplied on the upper floors and 46.0 m^2 of filter surface area on the ground floor. This is consistent with the filter surface area that could be incorporated into a new shelter in front of a cave, but exceeds the amount of filter surface area that can be incorporated into the historical wooden building in front of Cave 6.

ing a collective projected cross sectional area of 1 cm^2 have deposited onto each cm^2 of interior horizontal surface.

Case 2 of Table 2 shows the amount of protection afforded to the cave temple just by the existence of the wooden temple structure in front of the cave entrances. In this case, Cave 6 is modeled as it was operated by the Grottoes staff during the April 1991 experiment with the main ground-floor entrance doors to the cave temple open during the day but closed at night and with several doors on the upper floors of the building left open to the outdoors. Flows were calculated

using the computer model described earlier, and we see that the effect of the wooden temple front as it is operated today compared to base case 1 is to reduce the particle mass deposited onto horizontal surfaces in Cave 6 by about 47 percent. This occurs due to reduction of air flow through the cave temple due to the presence of extra pressure drops in the air path caused by the structure itself; there is no particle removal by filtration in this case.

Case 3 in Table 2 shows the amount of control that one would exercise if the doors at the ground level as well as the balcony doors and/or

windows on the upper floors were kept closed at all times. Air flow in and out of the cave temple would then flow through the existing cracks around the door and window panels. Our model calculates that in this case the average flow of air into Cave 6 under April 15–16, 1991, conditions would be 26 m^3 min^{-1} as opposed to 99 m^3 min^{-1} for the cave temple as it is operated today with doors open during the day but closed at night and with several door panels left open on the upper floors, and 317 m^3 min^{-1} for the case if the wooden temple front building did not exist. If all doors in the present building are kept closed at all times, particle deposition onto horizontal surfaces within the cave temple is reduced by about 81% relative to the base case.

We turn our attention next to the passive filtration alternative. In this case filter material would be placed into the door and window panels that exist around the surface of the wooden shelter in front of Cave 6. Here we identify three separate cases: cases 4, 5, and 6.

In case 4, we assume that the paper currently installed in the building's window panes, door panels at the ground floor, and third-floor levels will be removed and will be replaced by filter material. This has the added advantage that it does not change the external appearance of the building. Thus, the area available for the installation of filter material was taken to be equal to 2.56 m^2 each for both the downstairs and the upper levels of the wooden building front. We further assume that the doors and windows of the building are kept shut at all times, but we still allow for leakage of outdoor air into the building through cracks around the doors and window panels. The results of this case are shown in Table 2, case 4. We see that the mass deposition flux to horizontal surfaces is now 45 mg m^{-2} day^{-1} compared to the 262 mg m^{-2} day^{-1} for the base case. In other words, 17% of the mass of deposited particles relative to the base case still remains. The reason for this becomes evident when one examines the flow of air into the cave presented in Table 2, case 4: of the 34 m^3 min^{-1} of air that enters the

cave in this case, 24 m^3 min^{-1} or about 71% of the flow into the cave still passes through the cracks in the building shell (and, therefore, is not filtered) and only the remaining 29% of the flow passes through the filter material.

Case 5 is similar to the previous case with the only exception that we force all the air that enters the cave to pass through the filters. This could be achieved by caulking all the cracks and openings in the wooden temple building shell while still allowing only 2.56 m^2 of GSB-30 filter material to be placed in both the upstairs and ground-floor surfaces of the existing door and window panels of the temple front. The flow of air into the cave is reduced to about 6.3 m^3 min^{-1}. As a result, the mass of particles deposited onto horizontal surfaces within the cave is only 3.4 mg m^{-2} day^{-1} (Table 2, case 5), or about 1% of base case 1.

The Yungang Grottoes unfortunately suffer from water seepage through the sandstone cliff in addition to the particle deposition problem. Water condensation onto the rock sculptures within the caves is harmful as it promotes conversion of the surface of the stone to soft kaolin. The water vapor that enters Cave 6 in this manner presently is exhausted from that cave temple by the natural convection air flows that currently exist at Yungang, about 99 m^3 min^{-1} as shown in case 2 of Table 2. Reducing this air flow rate by a factor of almost 16 as suggested by case 5 above could cause problems arising from the inability to effectively remove the water vapor from the cave. Therefore, an ability to move air through the cave temples at volumes like those observed historically may be desirable. This can be achieved if the cross-sectional area available for placement of filter material in the surface of the building panels is increased. This may not be achieved easily at Cave 6, especially considering the historical character of the present wooden temple front building. Provision for installation of greater amounts of filter material could be made more easily in new shelters that are being designed for installation in front of caves that currently lack any protection. A preliminary study of such a shelter has been preformed

by Sedlak (1991). That design allows for a maximum surface area for filter placement in the face of a building the size of the one in front of Cave 6 of 46 m^2 and 55.4 m^2 in the ground level and upper level floors respectively. Such a possibility is examined in case 6 in Table 2. It is assumed that the dimensions of the cave would be the same as those for Cave 6 and that there will be no appreciable air leakage between the panels. To eliminate infiltration of untreated air as the doors are opened and closed, air locks would be installed. Using this greater exposed area of filter material with its associated lower resistance to air flow, the model predicts that $86 \text{ m}^3 \text{ min}^{-1}$ of air would enter the cave temple on average. In this case only 3% of the particle mass flux will deposit onto horizontal surfaces inside the cave temple relative to the case where a cave exists that has no wooden structure in front of it. Also, the time needed to cover completely an upward-facing horizontal surface inside the cave with the first monolayer of deposited dust would be increased to 6.3 years under conditions like those observed on April 15–16, 1991.

CONCLUSIONS

Passive air filtration systems that operate without the use of mechanical fans can be designed that can remove airborne particulate matter from the air that flows through certain buildings that are ventilated by natural convection flows. The design procedure for these systems links a natural convection-driven heat transfer model for air exchange through the building to an indoor air quality model that predicts indoor particle size distributions and particle fluxes onto surfaces. Example calculations worked for the case of particle filtration from the environment of an important Buddhist Cave Temple in China show that approximately 97% reduction in coarse particle deposition within that temple interior would be obtained while maintaining air exchange rates at near historical levels if sufficient surface area is made available for placement of filter material in the exterior walls of a shelter surrounding the temple structure. Such passive filtration systems may have important applications within historic buildings that cannot be refitted with mechanical fans and ductwork or in many locations worldwide where the reliable electric power needed to maintain a mechanical HVAC system is not available.

References

Christoforou, C. S., Salmon, L. G., and Cass, G. R. (1996a). Air Exchange within the Buddhist Cave Temples at Yungang, China. *Atmos. Environ.* 30:3995–4006.

Christoforou, C. S., Salmon, L. G., and Cass, G. R. (1996b). Fate of Atmospheric Particles within the Buddhist Cave Temples at Yungang, China. *Environ. Sci. Technol.*, 30:3425–3434.

Christoforou, C. S., Salmon, L. G., and Cass, G. R. (1994). Deposition of Atmospheric particles within the Buddhist Cave temples at Yungang, China. *Atmos. Environ*. 28:2081–2091.

Davies, C. N. (1979). Particle-fluid interaction. *J. Aerosol Sci*. 10:477–513.

Gelbard, F., and Seinfeld, J. H. (1980). Simulation of multicomponent aerosol dynamics. *J. Colloid Int. Sci.* 78:485–501.

Hancock, R. P., Esmen, N. A., and Furber, C. P. (1976). Visual response to dustiness. *J. Air Pollut. Control Assoc.* 26:54–57.

Jennings, B. H., and Lewis, S. R. (1965). *Air Conditioning and Refrigeration*, 4th ed. International Textbook Company, Scranton, PA, Chapter 12.

Minnesota Mining and Manufacturing Co., Filtration Products. (1993). Publication No. 70-0702-3443-3. St. Paul, MN.

Nazaroff, W. W., and Cass, G. R. (1991). Protecting museum collections from soiling due to the

deposition of airborne particles. *Atmos. Environ.* 25A:841–852.

Nazaroff, W. W., and Cass, G. R. (1989a). Mathematical modeling of indoor aerosol dynamics. *Environ. Sci. Technol.* 23:157–166.

Nazaroff, W. W., and Cass, G. R. (1989b). Mass transport aspects of pollutant removal at indoor surfaces. *Environ. Int.* 15:567–584.

Nazaroff, W. W., and Cass, G. R. (1987). Particle deposition from a natural convection flow onto a vertical isothermal flat plate. *J. Aerosol Sci.* 18: 445–455.

Sabersky, R. H., Acosta, A. J., and Hauptmann, E. G. (1989). *Fluid Flow, A First Course in Fluid Mechanics*, 3rd ed. Macmillan, New York, Chapter 3.

Salmon, L. G., Christoforou, C. S., and Cass, G. R. (1994). Airborne pollutants in the Buddhist cave temples at the Yungang Grottoes, China. *Environ. Sci. Technol.* 28:805–811.

Sedlak, V. (1991). *Report on a conceptual design study for a protective portico/facade for Cave 19 Yungang Grottoes, Shanxi province, PRC*. Vinzenz Sedlak Proprietary Limited, Randwick, New South Wales, Australia.